

Feasibility of optical probing of relativistic plasma singularities

Timur Zh. Esirkepov¹, Jie Mu², Yanjun Gu², Tae Moon Jeong², Petr Valenta², Ondrej Klimo², James K. Koga¹, Masaki Kando¹, Georg Korn², Sergei V. Bulanov^{1,2}, Alexander S. Pirozhkov¹

¹Kansai Photon Science Institute, National Institutes for Quantum and Radiological Science and Technology, 8-1-7 Umemidai, Kizugawa-city, Kyoto 619-0215, Japan

²Institute of Physics of the ASCR, ELI Beamlines Project, Na Slovance 2, 18221 Prague, Czech Republic

Abstract. Singularities in multi-stream flows of relativistic plasmas can efficiently produce coherent high-frequency radiation, as exemplified in the concepts of Relativistic Flying Mirror [S. V. Bulanov, *et al.*, *Phys. Rev. Lett.* **91**, 085001 (2003)] and Burst Intensification by Singularity Emitting Radiation (BISER) [Pirozhkov, *et al.*, *Scientific Reports* **7**, 17968 (2017)]. Direct observation of these singularities is challenging due to their extreme sharpness (tens of nanometers), relativistic velocity, and transient non-local nature. We propose to use ultrafast (a few light cycles) optical probe for identifying relativistic plasma singularities. Our Particle-in-Cell (PIC) simulations show that this diagnostic is feasible.

Introduction

Singularities easily form in multi-stream flows; they appear as crests or surges in some physical parameter, which is usually continuous, e.g., density, pressure, etc. If these crests and surges correspond to structurally stable singularities, they are inevitable and robust with respect to modulations, as explained by the catastrophe theory [1, 2]. In relativistic underdense plasmas driven by intense femtosecond lasers, two particularly interesting examples of the cusp singularities appear in electron density: one in a breaking wake wave [3] and another at the joining of the cavity wall and the bow wave [4]. In order to create these singularities, the driving laser should be sufficiently intense, with the dimensionless amplitude of the order of 1 or greater, $a_0 = eE_0/m_e c\omega_0 = (I_0/I_R)^{1/2} \gtrsim 1$, and short, with the length comparable to or shorter than the Langmuir wavelength, $c\tau \lesssim \lambda_{pe}$. Here c is the speed of light in vacuum, τ is the pulse duration; E_0 , I_0 , λ_0 and ω_0 are the laser electric field, irradiance, wavelength and angular frequency, respectively; e and m_e are the electron charge and mass, respectively; $I_R = \pi c^5 m_e^2 / 2e^2 \lambda_0^2 \approx 1.37 \times 10^{18} \text{ W/cm}^2 \times (\lambda_0[\mu\text{m}])^{-2}$ for a linearly polarized field; $\lambda_0[\mu\text{m}]$ denotes the wavelength in micrometres. We consider underdense plasma, with initial electron density much less than the critical density, $n_e \ll n_{cr}$, where $n_{cr} = m_e \omega_0^2 / 4\pi e^2 \approx 1.1 \times 10^{21} \text{ cm}^{-3} / (\lambda_0[\mu\text{m}])^2$.

The first mentioned above cusp singularity appears when a wake wave driven by relativistically intense laser pulse breaks. Under optimum conditions, this cusp can take a form of dense, thin shell moving behind the driving laser pulse with relativistic velocity. Due to the high density and sharpness, this shell can act as a Relativistic Flying Mirror, reflecting counter-propagating laser pulse [5-8]. The frequency of the reflected light is upshifted and duration shortened due to the double Doppler effect, so that a high-frequency coherent pulse is produced; in addition, the shell can have a concave, nearly parabolic, shape [6], which focuses reflected radiation to a tiny spot, promising record intensities [6, 9] beyond capabilities

of directly focused lasers. The Relativistic Flying Mirror was demonstrated experimentally in [10-17], where the frequency upshift was sufficient to convert a near infra-red laser radiation ($\lambda_0 \approx 0.8 \mu\text{m}$) to coherent soft x-rays, down to $\lambda_x = 7 \text{ nm}$.

The second mentioned cusp singularity appears when the bow wave detaches from the cavity wall, which happens when the laser spot is sufficiently narrow, $d < d_{\text{BW}} = 2\lambda_0(a_0 n_{\text{cr}}/n_e)^{1/2}/\pi$ [4]. This can be achieved, for example, due to relativistic self-focusing [18-20], where the spot size under stationary conditions can be estimated as [21] $d_0 = \lambda_0(a_0 n_{\text{cr}}/n_e)^{1/2}/\pi$ and the dimensionless amplitude as $a_0 = (8\pi P_0 n_e/P_c n_{\text{cr}})^{1/3}$, where the laser power P_0 exceeds the threshold $P_{\text{SF0}} = P_c (n_{\text{cr}}/n_e)$ and $P_c = 2m_e^2 c^5/e^2 \approx 0.017 \text{ TW}$ [20]. This cusp singularity is situated near the laser pulse head, and is strongly driven by the laser field. The accelerated motion of the electrons in the singularity leads to high-frequency radiation, while the singularity sharpness ensures constructive interference, producing bright coherent x-ray pulse [17, 22-27] termed Burst Intensification by Singularity Emitting Radiation (BISER) [28]. BISER has an unprecedentedly small source size: sub- μm measured directly (limited by the resolution of employed x-ray optics) and down to 10 nm predicted by the PIC simulations [28]. Together with the attosecond duration (predicted by PIC) and large photon number (measured 10^{10} photons with energy from 60 to 100 eV), this gives the peak spectral brightness of up to 10^{27} photons/ $\text{mm}^2 \text{ mrad}^2 \text{ s}$ 0.1% BW, among the highest amongst laser-based sources.

Direct experimental observation of these singularities is challenging due to their small size, relativistic velocity, and transient non-local nature. Here we propose to use ultrashort-duration (few-cycle) optical probe to detect these singularities. We specify the necessary probe pulse parameters and present the results of Particle-In-Cell (PIC) simulations to demonstrate the diagnostic feasibility.

Schlieren imaging scheme

A possible experimental setup is shown in Fig. 1. An intense driver laser pulse (further – the driver) with the dimensionless amplitude of $a_0 > 1$ is focused onto a supersonic gas jet. Since the magnitude of the driver field well exceeds that of the intra-atomic field, the gas becomes ionized with a time period shorter than the laser cycle. An underdense plasma is created. The driver power is greater than the threshold of relativistic self-focusing. The self-focusing driver excites a wake wave and bow wave, as seen below in the simulations. As described in Introduction, the cusps formed near the driver head emit radiation, BISER. It can be seen by an x-ray spectrometer placed within a relatively small angle about the direction of the driver propagation.

A weak probe laser pulse (further – the probe) is sent onto plasma in the transverse direction, perpendicularly to the driver axis. It propagates through the channel created by the driver, then goes into a special optical system which makes a Schlieren image as shown in Fig. 2. The probe is diffracted on singularities of electron density and electron current density, formed in plasma by the driver. These singularities are strongly localized, thus they easily break the approximation of geometric optics. As seen in Fig. 2, each singularity produces a spherical wave, which is imaged by the lens as a point-like source. In this way the singularities can be identified using Schlieren imaging. We note that the probe pulse length must be shorter than the longitudinal and *transverse* distances between singularities, $c\tau < d_0$, otherwise the spherical waves appear with their centers significantly drifting with time, so that different singularities become indiscernible due to the longitudinal and transverse motion blurs.

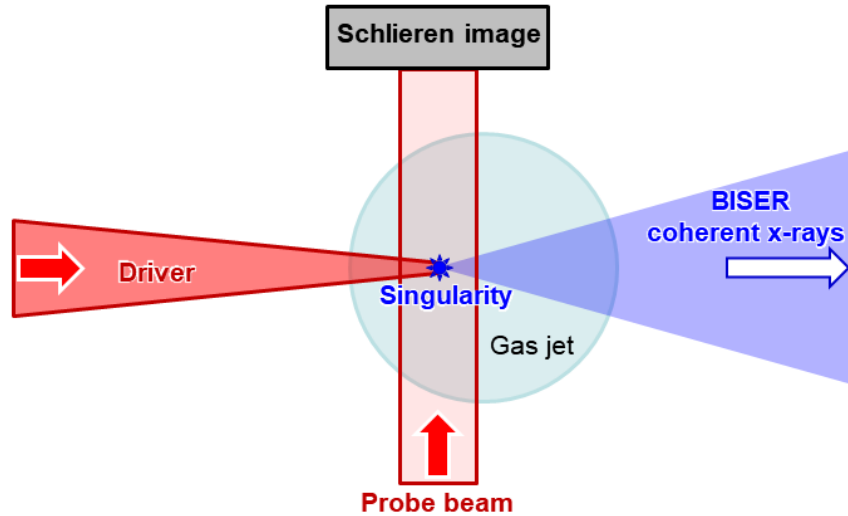


Fig. 1. The proposed experiment setup. The driver laser pulse is focused onto a gas jet. The resulting BISER is detected in the direction of the driver. The singularities are imaged by the probe ultrashort laser pulse with the same wavelength but different polarization.

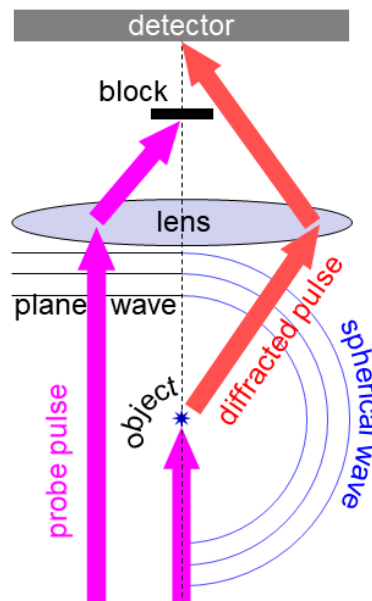


Fig. 2. The principal scheme of the Schlieren imaging. On the left: the rays and wave fronts of the probe pulse; after transmission through the lens the probe pulse is blocked by an opaque filter. On the right: the rays and wave fronts of the probe pulse diffracted at a point object; after transmission through the lens the diffracted pulse is focused onto the detector, forming the image of the object. The actual configuration has rotational symmetry with respect to the axis denoted by the dashed line.

We can roughly estimate the cusp singularity effect on the probe phase by assuming a stationary cusp density distribution $n_e = n_0(y/\lambda)^{-2/3}$ and integrating the refractive index difference: $\Delta\phi = (2\pi/\lambda)\int(n-1)dy$, where the refractive index is $n = (1-n_e/n_{cr})^{0.5}$. The integration from 0 to $y_{\max} = M\lambda$ gives the real part

$\text{Re}[\Delta\phi] = 2\pi((M^{2/3} - n_0/n_{cr})^{3/2} - M)$, which slowly diverges as $\text{Re}[\Delta\phi] \rightarrow -3\pi M^{1/3}n_0/n_{cr}$ at large M . We note that in 3D the density starts to decrease quickly at $y > d_0$, so for estimate we can use $M = d_0/\lambda$. The imaginary part is $\text{Im}[\Delta\phi] = 2\pi(n_0/n_{cr})^{3/2}$, corresponding to the transmission intensity of $\exp(-2\pi(n_0/n_{cr})^{3/2})$. For the cusp parameters as in [29] ($n_0 = 0.023n_{cr}$) this gives the real part of $\text{Re}[\Delta\phi] = -0.46$ radian, and the imaginary part of $\text{Im}[\Delta\phi] = 0.02$ rad, corresponding to the beam transmission of 0.96, i.e. 4% attenuation. Such phase shift and attenuation are well within the measurable ranges.

Simulation setup

We have performed two-dimensional (2D) PIC simulations using the REMP code [30]. The setup is shown in Fig. 3. The driver laser pulse propagates in the direction of x -axis (in Fig. 3 – from the left to the right); it is p -polarized, i. e. in the direction of y -axis, in the plane of the simulation box; initially its electromagnetic field is given by E_x, E_y, B_z components while other components are zero. The driver has gaussian shape with the full width at half maximum (FWHM) of $5\lambda_0$ and the focal spot size of $5\lambda_0$. Here λ_0 is the driver wavelength. The driver amplitude is $a_0 = 6.6$; its assumed focal plane is inside plasma at the distance of $40\lambda_0$ from the vacuum-plasma interface, where the driver enters plasma (“assumed”, because the value is given for the case of the driver propagation in vacuum).

The plasma slab is rectangular and has the sizes of $160\lambda_0$ and $80\lambda_0$ in the direction of x and y axes, respectively. The electron density is $n_e = 0.01 n_{cr}$.

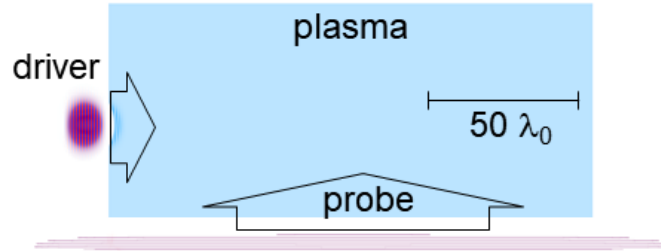


Fig. 3. The PIC simulation setup.

The probe laser pulse propagates in the direction of y -axis (in Fig. 3 – from the bottom to the top); it is s -polarized, i. e. in the direction of z -axis, perpendicularly to the plane of the simulation box. The difference in the driver and probe polarization helps to distinguish the evolution of the driver and probe. As it is well known, the interaction of p -polarized electromagnetic wave with plasmas has special symmetry in 2D configuration: if only three components of electromagnetic field, E_x, E_y, B_z , and only two components of plasma particles momentum, p_x, p_y , were initially non-zero, then all other components will be zero forever. Thus, in the interaction of p -polarized driver with initially calm plasma, the components E_z, B_x, B_y can acquire non-zero values only in the presence of the s -polarized probe. The probe has Gaussian shape with the FWHM length of $3\lambda_0$ and the focal spot size of $160/3\lambda_0$. Its amplitude is $a_0 = 0.01$; its assumed focal plane is at the bottom plasma-vacuum interface (for such a wide probe, its Rayleigh length is much greater than the transverse extent of the plasma slab). The probe is sent to plasma 50 laser cycles later than the driver, so that the probe propagates through the wake wave when the driver is approximately at the center of the plasma slab. The mesh size is $\lambda_0/16$ in both spatial directions, which is

sufficient to see the second harmonic. The time step is 0.999 of the threshold corresponding to the Courant-Friedrichs-Lewy condition. The number of quasi-particles per cell is 1; plasma consists of electrons with the neutralizing background of immobile ions.

Simulation results

The results of simulations are presented in Figs. 4-6. In the figures, the time unit is the laser cycle. The driver and probe pulses enter plasma approximately at $t=20$ and $t=70$, respectively. In the figures the probe pulse is represented in two ways simultaneously. The nearly horizontal red curves are the contours of the E_z field component of the probe corresponding to the value of $E_z=0.001$ (in terms of dimensionless amplitude). The white-red color-scale shows the spatial distribution of the magnitude of the difference between the values of the E_z field component of the probe calculated in two simulations: in one simulation both the driver and the probe pulse are present, in another simulation only the probe pulse is present. This method allows to get rid of physical, but undesirable, reflection of the probe from the plasma slab boundaries. In addition, the Fourier filter was applied to remove the wave propagating at 90° , similarly to the blocking technique in the Schlieren imaging.

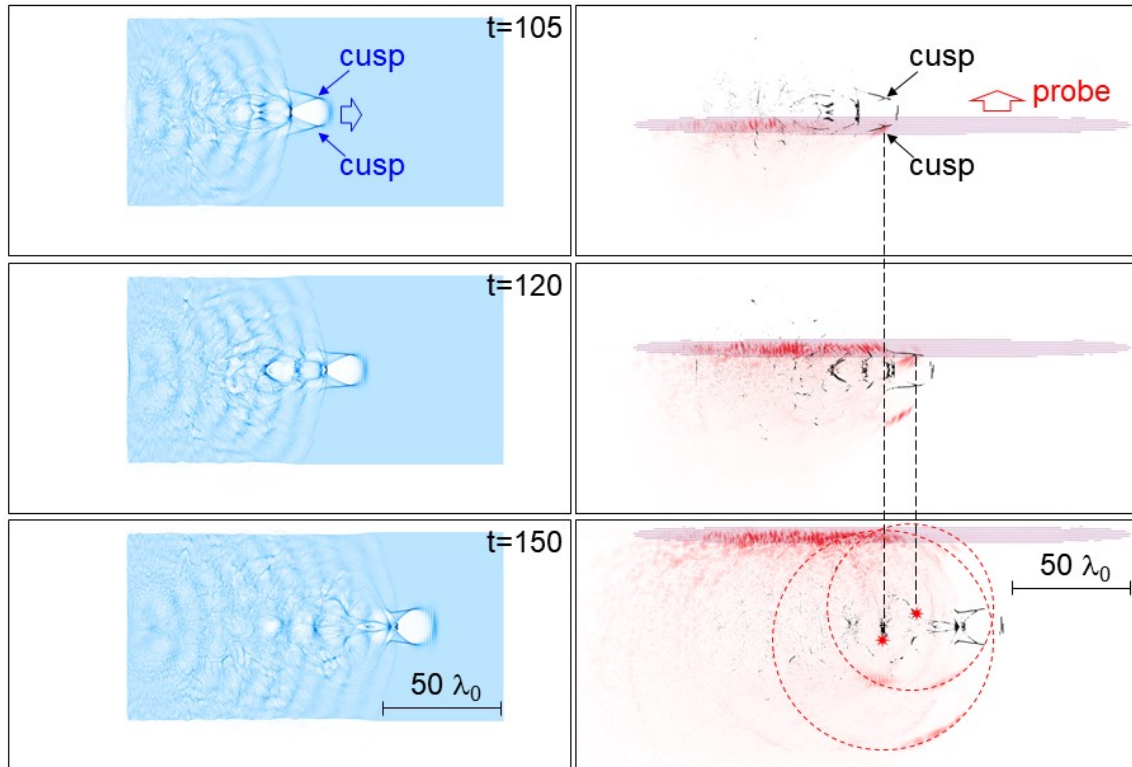


Fig. 4. On the left: electron density at different moments of time (the time unit is the laser cycle). The driver pulse can be traced by density modulations at the front of the first cavity of the wake wave. On the right: black curves are for the electron density (at the levels of density 3 and 4 times greater than the initial density); nearly horizontal red curves are for the electric field of the probe; the white-red color-scale is for the absolute difference of the E_z field component between two simulations, one with the driver and probe and another with the probe only; the waves going at 90° are filtered out (similarly to the Schlieren imaging) using Fourier filter.

In Fig. 4, one can easily see distortions in the probe transmitted through the wake wave. These distortions are "enriched" by spherical fronts which originate at various singularities appearing in the wake wave. We can identify the singularities formed due to longitudinal and transverse wave breaks. The most prominent diffraction, however, occurs at the cusps near the head of the driver pulse. The corresponding spherical wave fronts can be collected by the lens and form the Schlieren image of the cusps, as in Fig. 2. We note that the cusps move with the group velocity of the driver pulse, which is close to the speed of light in vacuum, c . Therefore the image of the two cusps will be such as if the cusps were slightly rotated with respect to each other, a manifestation of the Penrose-Terrell effect.

Figs. 5 and 6 show the probe pulse propagation through the wake wave, so one can see where the probe diffraction occurs and how the spherical waves are formed from individual acts of diffraction. In addition, the spatial spectrum of the E_z field component of the probe is shown at different times. The circle $k_x^2+k_y^2=1$ corresponds to waves with the wavelength of λ_0 going to all possible directions. This circle appears very early due to diffraction of the probe on density modulations at the plasma-vacuum interface.

In Figs. 5 and 6, one can see the appearance of characteristic "protrusions" corresponding to high-frequency waves, which correlate with the onset of diffraction at the cusps. The "protrusions" are the portions of an ellipse given by the formula $\omega/c = (k_x^2+k_y^2)^{1/2} = \omega_0/(1-\beta \cos \alpha)$, where β is the velocity of the cusp normalized by c , $\tan \alpha = k_y/k_x$. In the direction of the cusp motion, the diffracted wave frequency is upshifted due to the double Doppler effect, in the opposite direction it is downshifted. We note that even though the frequency gets upshifted and downshifted in different directions, the diffracted wave fronts are spherical. The diffraction on cusps can be considered both as transmission in the direction of the probe and as reflection in different directions. The reflection from relativistic cusps will be described soon elsewhere.

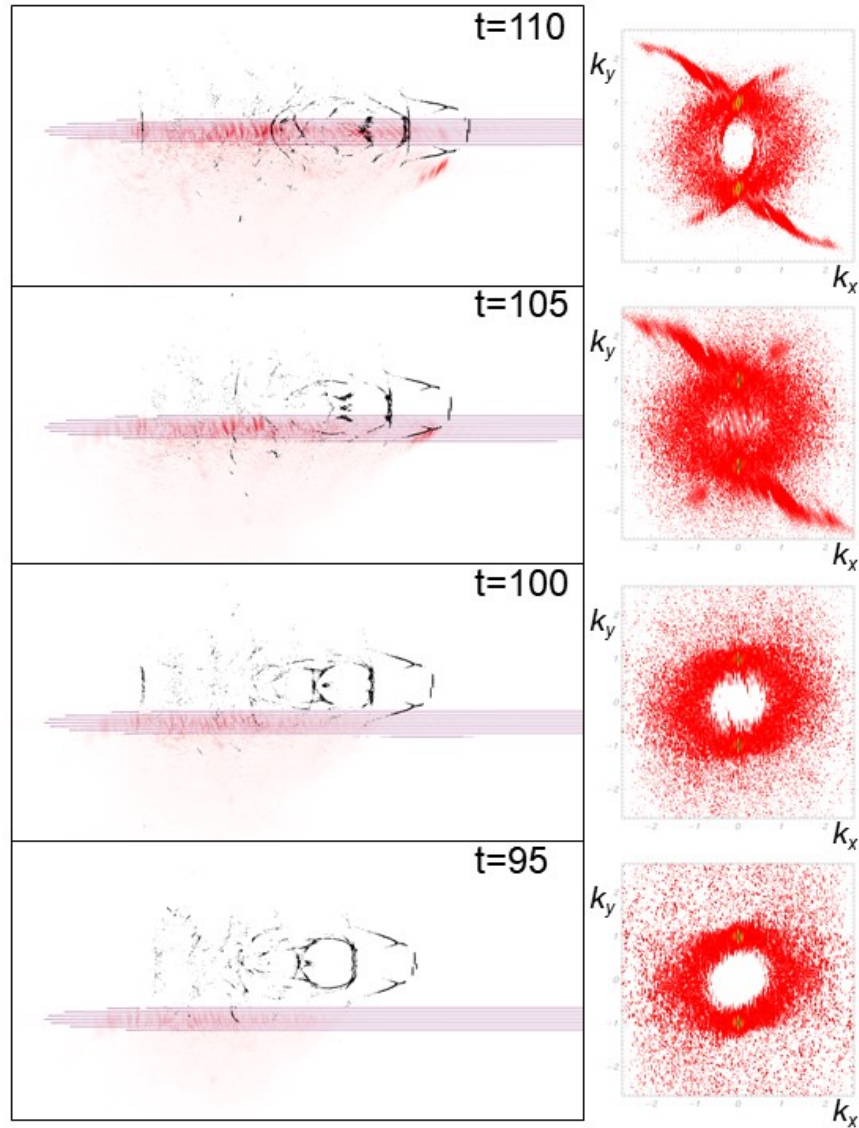


Fig. 5. On the left: the probe propagation through the wake wave; the curves and color-scale are the same as in Fig. 4. On the right: the magnitude of the spatial spectrum of the E_z field component of the probe at the same instances of time as the spatial distributions on the left. The spectral magnitude has maxima at two bright spots at $k_x=0$ and $k_y=\pm 1$, which correspond to initial probe beam direction and laser wavelength λ_0 . The appearance of high-frequency “protrusions” out of the circle $k_x^2+k_y^2=1$ correlates with the onsets of diffraction from the cusps. The “protrusions” are the portions of an ellipse.

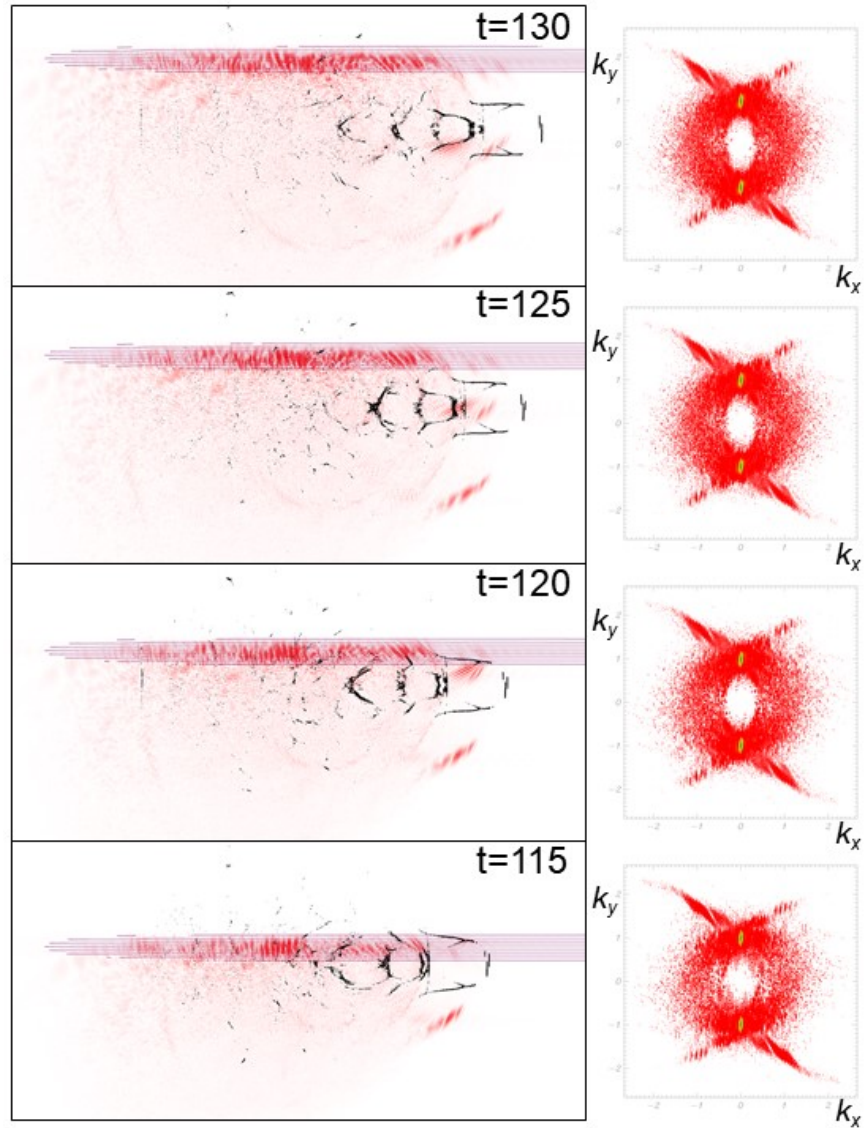


Fig. 6. The continuation of the time sequence of Fig. 5.

Conclusion

Using analytical estimates and 2D PIC simulations we show that the Schlieren imaging of relativistically moving singularities in laser plasma is feasible. We derive the required duration of the optical probe pulse ensuring discernibility of different singularities in the images.

Acknowledgements

We thank David Neely for discussions. We acknowledge financial support from the QST Director Fund 創成的研究 20.

References

1. V. I. Arnold, *Catastrophe theory*, 3rd ed. (Springer-Verlag, Berlin Heidelberg New York, 1992).
2. T. Poston and I. Stewart, *Catastrophe theory and its applications*. (Dover Pubns, Mineola, NY, USA, 1996).
3. S. V. Bulanov, F. Pegoraro, A. M. Pukhov, and A. S. Sakharov, "Transverse-Wake Wave Breaking," *Phys. Rev. Lett.* **78**, 4205-4208 (1997).
4. T. Z. Esirkepov, Y. Kato, and S. V. Bulanov, "Bow Wave from Ultraintense Electromagnetic Pulses in Plasmas," *Phys. Rev. Lett.* **101**, 265001-4 (2008).
5. S. V. Bulanov, I. N. Inovenkov, V. I. Kirsanov, N. M. Naumova, and A. S. Sakharov, "Electromagnetic Radiation Frequency Upshift upon Interaction with Nonlinear Plasma Waves," *Sov. Phys.-Lebedev Inst. Rep.*, 9-11 (1991).
6. S. V. Bulanov, T. Z. Esirkepov, and T. Tajima, "Light intensification towards the Schwinger limit," *Phys. Rev. Lett.* **91**, 085001-4 (2003).
7. S. V. Bulanov, T. Z. Esirkepov, M. Kando, A. S. Pirozhkov, and N. N. Rosanov, "Relativistic mirrors in plasmas. Novel results and perspectives," *Phys. Usp.* **56**, 429-464 (2013).
8. M. Kando, T. Z. Esirkepov, J. Koga, A. S. Pirozhkov, and S. V. Bulanov, "Coherent, Short-Pulse X-ray Generation via Relativistic Flying Mirrors," *Quantum Beam Sci.* **2**, 9 (2018).
9. T. Z. Esirkepov, S. V. Bulanov, M. Kando, A. S. Pirozhkov, and A. G. Zhidkov, "The flying mirror: future brightest x-ray and gamma-ray source," *Proc. SPIE* **7359**, 735909-11 (7 May 2009), (*Proc. Harnessing Relativistic Plasma Waves as Novel Radiation Sources from Terahertz to X-Rays and Beyond*, Prague, Czech Republic, 22 April 2009, edited by D. A. Jaroszynski and A. Rousse).
10. M. Kando, Y. Fukuda, A. S. Pirozhkov, J. Ma, I. Daito, L. M. Chen, T. Z. Esirkepov, K. Ogura, T. Homma, Y. Hayashi, H. Kotaki, A. Sagisaka, M. Mori, J. K. Koga, H. Daido, S. V. Bulanov, T. Kimura, Y. Kato, and T. Tajima, "Demonstration of laser-frequency upshift by electron-density modulations in a plasma wakefield," *Phys. Rev. Lett.* **99**, 135001-4 (2007).
11. A. S. Pirozhkov, J. Ma, M. Kando, T. Z. Esirkepov, Y. Fukuda, L. M. Chen, I. Daito, K. Ogura, T. Homma, Y. Hayashi, H. Kotaki, A. Sagisaka, M. Mori, J. K. Koga, T. Kawachi, H. Daido, S. V. Bulanov, T. Kimura, Y. Kato, and T. Tajima, "Frequency multiplication of light back-reflected from a relativistic wake wave," *Phys. Plasmas* **14**, 123106-22 (2007).
12. A. S. Pirozhkov, T. Z. Esirkepov, M. Kando, Y. Fukuda, J. Ma, L. M. Chen, I. Daito, K. Ogura, T. Homma, Y. Hayashi, H. Kotaki, A. Sagisaka, M. Mori, J. K. Koga, T. Kawachi, H. Daido, S. V. Bulanov, T. Kimura, Y. Kato, and T. Tajima, "Demonstration of light reflection from the relativistic mirror," *Journal of Physics: Conference Series* **112**, 042050-4 (12 Jun 2008), (*Proc. IFSA 2007*, Kobe, Japan, 9-14 September 2007, edited by H. Azechi, B. Hammel, and J.-C. Gauthier).
13. A. S. Pirozhkov, M. Kando, T. Z. Esirkepov, J. Ma, Y. Fukuda, L. M. Chen, I. Daito, K. Ogura, T. Homma, Y. Hayashi, H. Kotaki, A. Sagisaka, M. Mori, J. K. Koga, T. Kawachi, H. Daido, S. V. Bulanov, T. Kimura, Y. Kato, and T. Tajima, "Relativistic Tennis Using Flying Mirror," *AIP Conf. Proc.* **1024**, 37-51 (Jun 2008), (*Proc. Laser-Driven Relativistic Plasmas Applied for Science, Industry, and Medicine: The 1st International Symposium*, Kyoto (Japan), 17-20 September 2007, edited by P. R. Bolton, H. Daido, and S. V. Bulanov).
14. M. Kando, A. S. Pirozhkov, K. Kawase, T. Z. Esirkepov, Y. Fukuda, H. Kiriya, H. Okada, I. Daito, T. Kameshima, Y. Hayashi, H. Kotaki, M. Mori, J. K. Koga, H. Daido, A. Y. Faenov, T. Pikuz, J. Ma, L. M. Chen, E. N. Ragozin, T. Kawachi, Y. Kato, T. Tajima, and S. V. Bulanov, "Enhancement of Photon Number Reflected by the Relativistic Flying Mirror," *Phys. Rev. Lett.* **103**, 235003-4 (2009).
15. A. S. Pirozhkov, M. Kando, T. Z. Esirkepov, Y. Fukuda, L.-M. Chen, I. Daito, K. Ogura, T. Homma, Y. Hayashi, H. Kotaki, A. Sagisaka, M. Mori, J. K. Koga, T. Kawachi, H. Kiriya, H. Okada, K. Kawase, T. Kameshima, N. Nishimori, E. N. Ragozin, A. Y. Faenov, T. A. Pikuz, T. Kimura, T. Tajima, H. Daido, Y.

- Kato, and S. V. Bulanov, "Demonstration of Flying Mirror with Improved Efficiency," *AIP Conf. Proc.* **1153**, 274-284 (25 Jul 2009), (Proc. *2nd Int. Symp. Laser-Driven Relativistic Plasmas Applied to Science, Industry and Medicine*, Kyoto (Japan), 19-23 January 2009, edited by P. R. Bolton, H. Daido, and S. V. Bulanov).
16. M. Kando, A. S. Pirozhkov, Y. Fukuda, T. Z. Esirkepov, I. Daito, K. Kawase, J. L. Ma, L. M. Chen, Y. Hayashi, M. Mori, K. Ogura, H. Kotaki, A. Sagisaka, E. N. Ragozin, A. Faenov, T. Pikuz, H. Kiriyaama, H. Okada, T. Kameshima, J. K. Koga, K. Belyaev, F. F. Kamenets, A. Sugiyama, T. Kawachi, H. Daido, T. Kimura, Y. Kato, T. Tajima, and S. V. Bulanov, "Experimental studies of the high and low frequency electromagnetic radiation produced from nonlinear laser-plasma interactions," *Eur. Phys. J. D* **55**, 465-474 (2009).
 17. A. S. Pirozhkov, M. Kando, T. Z. Esirkepov, P. Gallegos, H. Ahmed, E. N. Ragozin, A. Y. Faenov, T. A. Pikuz, J. K. Koga, H. Kiriyaama, P. McKenna, M. Borghesi, K. Kondo, H. Daido, Y. Kato, D. Neely, and S. V. Bulanov, "Coherent x-ray generation in relativistic laser/gas jet interactions," *Proc. SPIE* **8140**, 81400A-16 (5 Oct 2011), (Proc. *X-Ray Lasers and Coherent X-Ray Sources: Development and Applications IX*, San Diego, California, USA 23-25 August 2011, edited by J. Dunn and A. Klisnick).
 18. G. A. Askaryan, "Effect of the gradient of a strong electromagnetic ray on electrons and atoms," *Zhur. Eksptl'. i Teoret. Fiz.* **42**, 1567-70 (1962).
 19. A. Litvak, "Finite-amplitude wave beams in a magnetoactive plasma," *Sov. Phys. JETP.* **30**, 344 (1970).
 20. G.-Z. Sun, E. Ott, Y. C. Lee, and P. Guzdar, "Self-focusing of short intense pulses in plasmas," *Phys. Fluids* **30**, 526-532 (1987).
 21. S. S. Bulanov, V. Y. Bychenkov, V. Chvykov, G. Kalinchenko, D. W. Litzenberg, T. Matsuoka, A. G. R. Thomas, L. Willingale, V. Yanovsky, K. Krushelnick, and A. Maksimchuk, "Generation of GeV protons from 1 PW laser interaction with near critical density targets," *Phys. Plasmas* **17**, 043105-8 (2010).
 22. A. S. Pirozhkov, M. Kando, T. Z. Esirkepov, P. Gallegos, H. Ahmed, E. N. Ragozin, A. Y. Faenov, T. A. Pikuz, T. Kawachi, A. Sagisaka, J. K. Koga, M. Coury, J. Green, P. Foster, C. Brenner, B. Dromey, D. R. Symes, M. Mori, K. Kawase, T. Kameshima, Y. Fukuda, L. Chen, I. Daito, K. Ogura, Y. Hayashi, H. Kotaki, H. Kiriyaama, H. Okada, N. Nishimori, T. Imazono, K. Kondo, T. Kimura, T. Tajima, H. Daido, P. Rajeev, P. McKenna, M. Borghesi, D. Neely, Y. Kato, and S. V. Bulanov, "Soft-X-Ray Harmonic Comb from Relativistic Electron Spikes," *Phys. Rev. Lett.* **108**, 135004-5 (2012).
 23. T. Pikuz, A. Faenov, A. Pirozhkov, A. Astapov, G. Klushin, S. Pikuz, N. Nagorskiy, S. Magnitskiy, T. Esirkepov, J. Koga, T. Nakamura, S. Bulanov, Y. Fukuda, Y. Hayashi, H. Kotaki, Y. Kato, and M. Kando, "High performance imaging of relativistic soft X-ray harmonics by sub-micron resolution LiF film detectors," *Physica Status Solidi C* **9**, 2331-2335 (2012).
 24. A. S. Pirozhkov, M. Kando, T. Z. Esirkepov, P. Gallegos, H. Ahmed, E. N. Ragozin, A. Y. Faenov, T. A. Pikuz, T. Kawachi, A. Sagisaka, J. K. Koga, M. Coury, J. Green, P. Foster, C. Brenner, B. Dromey, D. R. Symes, M. Mori, K. Kawase, T. Kameshima, Y. Fukuda, L. Chen, I. Daito, K. Ogura, Y. Hayashi, H. Kotaki, H. Kiriyaama, H. Okada, N. Nishimori, T. Imazono, K. Kondo, T. Kimura, T. Tajima, H. Daido, P. Rajeev, P. McKenna, M. Borghesi, D. Neely, Y. Kato, and S. V. Bulanov, "High order harmonics from relativistic electron spikes," *New J. Phys.* **16**, 093003-30 (2014).
 25. A. S. Pirozhkov, M. Kando, T. Z. Esirkepov, P. Gallegos, H. Ahmed, E. N. Ragozin, A. Y. Faenov, T. A. Pikuz, T. Kawachi, A. Sagisaka, J. K. Koga, M. Coury, J. Green, P. Foster, C. Brenner, B. Dromey, D. R. Symes, M. Mori, K. Kawase, T. Kameshima, Y. Fukuda, L. M. Chen, I. Daito, K. Ogura, Y. Hayashi, H. Kotaki, H. Kiriyaama, H. Okada, N. Nishimori, T. Imazono, K. Kondo, T. Kimura, T. Tajima, H. Daido, P. Rajeev, P. McKenna, M. Borghesi, D. Neely, Y. Kato, and S. V. Bulanov, "Relativistic high harmonic generation in gas jet targets " *AIP Conf. Proc.* **1465**, 167-171 (11 Jul 2012), (Proc. *The 3rd International Symposium "Laser-Driven Relativistic Plasmas Applied to Science, Energy, Industry, and Medicine"*, Kyoto, Japan, 30 May - 2 June 2011, edited by S. V. Bulanov, A. Yokoyama, Y. I. Malakhov, and Y. Watanabe).

26. A. S. Pirozhkov, T. Z. Esirkepov, T. A. Pikuz, A. Y. Faenov, K. Ogura, Y. Hayashi, H. Kotaki, E. N. Ragozin, D. Neely, H. Kiriyaama, J. K. Koga, Y. Fukuda, A. Sagisaka, M. Nishikino, T. Imazono, N. Hasegawa, T. Kawachi, H. Daido, Y. Kato, S. V. Bulanov, K. Kondo, and M. Kando, "High-Order Harmonic Generation by Relativistic Plasma Singularities: The Driving Laser Requirements," *Springer Proceedings in Physics* **202**, 85-92 (24 Feb 2018), (Proc. X-Ray Lasers 2016, Nara, Japan, 22-27 May 2016, edited by T. Kawachi, S. V. Bulanov, H. Daido, and Y. Kato).
27. A. S. Pirozhkov, T. Z. Esirkepov, T. A. Pikuz, A. Y. Faenov, A. Sagisaka, K. Ogura, Y. Hayashi, H. Kotaki, E. N. Ragozin, D. Neely, J. K. Koga, Y. Fukuda, M. Nishikino, T. Imazono, N. Hasegawa, T. Kawachi, H. Daido, Y. Kato, S. V. Bulanov, K. Kondo, H. Kiriyaama, and M. Kando, "Laser Requirements for High-Order Harmonic Generation by Relativistic Plasma Singularities," *Quantum Beam Sci.* **2**, 7 (2018).
28. A. S. Pirozhkov, T. Z. Esirkepov, T. A. Pikuz, A. Y. Faenov, K. Ogura, Y. Hayashi, H. Kotaki, E. N. Ragozin, D. Neely, H. Kiriyaama, J. K. Koga, Y. Fukuda, A. Sagisaka, M. Nishikino, T. Imazono, N. Hasegawa, T. Kawachi, P. R. Bolton, H. Daido, Y. Kato, K. Kondo, S. V. Bulanov, and M. Kando, "Burst intensification by singularity emitting radiation in multi-stream flows," *Scientific Reports* **7**, 17968 (10 pages) (2017).
29. A. S. Pirozhkov, T. Z. Esirkepov, T. A. Pikuz, A. Y. Faenov, K. Ogura, Y. Hayashi, H. Kotaki, E. N. Ragozin, D. Neely, H. Kiriyaama, J. K. Koga, Y. Fukuda, A. Sagisaka, M. Nishikino, T. Imazono, N. Hasegawa, T. Kawachi, P. R. Bolton, H. Daido, Y. Kato, K. Kondo, S. V. Bulanov, and M. Kando, "Burst intensification by singularity emitting radiation in multi-stream flows," *Scientific Reports* **7**, 17968-10 (2017).
30. T. Z. Esirkepov, "Exact charge conservation scheme for Particle-in-Cell simulation with an arbitrary form-factor," *Comput. Phys. Comm.* **135**, 144-153 (2001).